

# Methodology for the evaluation of yield strength and hardening behavior of metallic materials by indentation with spherical tip

Dejun Ma

*Department of Applied Physics and Materials Research Center, The Hong Kong Polytechnic University, Hung Hom, Kowloon, Hong Kong, People's Republic of China and Surface Engineering Research Institute, CMES, Beijing 10072, People's Republic of China*

Chung Wo Ong<sup>a)</sup>

*Department of Applied Physics and Materials Research Center, The Hong Kong Polytechnic University, Hung Hom, Kowloon, Hong Kong, People's Republic of China*

Jian Lu

*LASMAS, University de Technologie de Troyes, BP2060-10010 Troyes Cedex, France*

Jiawen He

*State Key Laboratory for Mechanical Behavior of Materials, Xi'an Jiaotong University, Xi'an 710049, People's Republic of China*

(Received 7 January 2003; accepted 15 April 2003)

This article presents a methodology for evaluating the yield strength and hardening behavior of metallic materials by spherical indentation. Two types of assumed material behaviors with a pure elastic-Hollomon's power law hardening and a pure elastic-linear hardening were considered separately in the models of spherical indentation. The numerical relationships between the material properties and indentation responses were established on the basis of dimensional and finite element analysis. As the first approximation to the real plastic flow properties, the yield strengths and hardening behaviors determined from the spherical indentation loading curve and the numerical relationships were used to derive the intersecting points between Hollomon's power law hardening curve and linear hardening line. Through proceeding the three parameter's regression analysis with Swift's power law function for the intersecting points determined at different maximum indentation depths, the final yield strength and hardening behavior of tested material can be obtained. The validation of this method was examined by investigating three groups of materials with near linear hardening behavior, near Hollomon's power law hardening behavior, and initial yield plateau. It is concluded that the proposed method is applicable to a wide variety of materials which exhibit separate hardening behaviors. © 2003 American Institute of Physics. [DOI: 10.1063/1.1579862]

## I. INTRODUCTION

Indentation experiments with continuous load-displacement curves measured by depth-sensing indentation technique have been widely used for determining the mechanical properties of materials with small dimension.<sup>1-7</sup> Both self-similar sharp indenter tip (like Vickers and Berkovich tips) and spherical indenter tip can be employed for this purpose. Generally, a sharp indenter tip is appreciable for the measurement of hardness, while a spherical one is favorable for the evaluation of the plastic flow properties, such as the yield strength and hardening behavior. The reason for the difference is associated with the different strain fields under these two kinds of indenters. The strain fields produced by a sharp indenter tip at different depths are self-similar, so the load-displacement curves with different depths are not able to reflect the plastic flow properties corresponding to different regions of the stress-strain relationship of a material. This makes it difficult to identify them from the continuous load-displacement curve.<sup>8</sup> On the contrary, the

geometrical topography of the strain fields beneath a spherical indenter tip would change all the way with increasing indentation depth. Correspondingly, more information on the plastic flow properties of material can be reflected in the indentation responses, and this provides the possibility to deduce them.<sup>9</sup>

A key to fulfill the aim of identifying the plastic flow properties is to establish the relationship between spherical indentation responses and the elastoplastic properties of indented material. To do this, the functional type of the uniaxial stress-strain relation of indented material has to be assumed, and it is usually taken as linear elasticity combined with Hollomon's power law hardening. Based on the hypothesis, the methods for determining the plastic flow properties of metallic materials have been proposed in recent years.<sup>10-12</sup> The advantage of these methods lies in their simplicity, however, a large error in evaluation for the mechanical properties, especially for the yield strength, may appear when the material is far from the assumed Hollomon's power law hardening behavior. This means that for the material to be measured with unknown hardening behavior, the yield strength determined by the reported methods is quite unreli-

<sup>a)</sup> Author to whom correspondence should be addressed; electronic mail: apacwong@inet.polyu.edu.hk

able. Thus, developing an approach to be applicable to wide materials showing very different hardening behaviors is crucial and also the aim of this work.

In this article, both Hollomon's power law and linear hardening behaviors are considered in the models of spherical indentation. Dimensional analysis and finite element calculations are applied to investigate the numerical relationships between spherical indentation responses and the material properties. By determining the first approximate yield strengths and hardening behaviors as well as the characteristic points defined in this article from the spherical indentation loading curve and the numerical relationships, the final estimation on yield strength and hardening behavior with small error for very different material behavior can be achieved.

## II. ANALYSIS OF SPHERICAL INDENTATION

Indentation is a complicated nonlinear process, which deals with elastoplastic material behavior, large strains and rotation, and variable contact condition. No analytical solution for indentation response is available. So numerical analysis appears to be necessary. In this study, finite element method (FEM) was employed to simulate the spherical indentation process. It is assumed that the spherical indenter is elastic. The contact interface between the indenter and indented material is free of friction. The tested material behaves as an isotropic and rate-independent solid, and obeys Von Mises yield criterion and pure isotropic hardening rule. In particular, two types of uniaxial stress-strain relations are assumed separately as material properties. The first one is elastic-Hollomon's power law hardening relation:

$$\sigma = \begin{cases} E\varepsilon & \varepsilon \leq \varepsilon_{yH} \\ \sigma_{yH}(\varepsilon/\varepsilon_{yH})^n & \varepsilon > \varepsilon_{yH} \end{cases} \quad (1)$$

where  $E$  is the Young's modulus,  $\sigma$  and  $\varepsilon$  are the true stress and true strain,  $\sigma_{yH}$  and  $\varepsilon_{yH} = \sigma_{yH}/E$  are the yield stress and yield strain, and  $n$  is the strain hardening exponent. The second one is elastic-linear hardening relation:

$$\sigma = \begin{cases} E\varepsilon & \varepsilon \leq \varepsilon_{yL} \\ \sigma_{yL} + K(\varepsilon - \varepsilon_{yL}) & \varepsilon > \varepsilon_{yL} \end{cases} \quad (2)$$

where  $\sigma_{yL}$  and  $\varepsilon_{yL} = \sigma_{yL}/E$  are corresponding yield stress and yield strain, and  $K$  is the strain hardening modulus.

As the important experimental data directly measured by depth-sensing indentation technique, the relationship of indentation load ( $P$ ) and depth ( $h$ ) in loading process can be regressed by using the following expression:

$$P = P_m(h/h_m)^X, \quad (3)$$

where  $h_m$  is the maximum indentation depth,  $P_m$  the fitting maximum load corresponding to  $h_m$ , and  $X$  the fitting exponent. In general, both  $P_m$  and  $X$  should be functions of the elastoplastic properties ( $E$ ,  $\sigma_{yH}$ ,  $n$  or  $E$ ,  $\sigma_{yL}$ ,  $K$ ) of tested material, the Young's modulus ( $E_i$ ) and radius ( $R$ ) of spherical indenter, and the maximum indentation depth ( $h_m$ ). Here the Poisson's ratios of indented material and indenter are assumed as constants of 0.3 and 0.2, so they do not appear in

TABLE I. Values or ranges of parameters used in finite element calculations.

$E$ (GPa)	$R$ ( $\mu\text{m}$ )	$\sigma_{yH}$ or $\sigma_{yL}$ (MPa)	$n$	$K$ (MPa)	$E_i$ (GPa)	$h_m$ ( $\mu\text{m}$ )
70	100	30–800	0–0.375	0–6000	70–1120	1–5

the functions. Corresponding to the two different kinds of hardening behaviors mentioned above, the functions of  $P_m$  and  $X$  can be expressed respectively as:

$$P_m = P_{mH}(E, \sigma_{yH}, n, E_i, R, h_m), \quad (4)$$

$$X = X_H(E, \sigma_{yH}, n, E_i, R, h_m) \quad (5)$$

and

$$P_m = P_{mL}(E, \sigma_{yL}, K, E_i, R, h_m), \quad (6)$$

$$X = X_L(E, \sigma_{yL}, K, E_i, R, h_m). \quad (7)$$

By applying  $\Pi$  theorem of dimensional analysis, functions (4)–(7) can be rewritten in dimensionless form:

$$P_m/(ER^2) = \Phi_H(\sigma_{yH}/E, n, E_i/E, h_m/R), \quad (8)$$

$$X = \Psi_H(\sigma_{yH}/E, n, E_i/E, h_m/R) \quad (9)$$

and

$$P_m/(ER^2) = \Phi_L(\sigma_{yL}/E, K/E, E_i/E, h_m/R) \quad (10)$$

$$X = \Psi_L(\sigma_{yL}/E, K/E, E_i/E, h_m/R). \quad (11)$$

For definite quantities  $\sigma_{yH}$ ,  $\sigma_{yL}$ ,  $n$ ,  $K$ ,  $E$ ,  $E_i$ ,  $R$ , and  $h_m$ ,  $P_m/(ER^2)$  and  $X$  can be determined from finite element calculations based on the commercial code ABAQUS.<sup>13</sup> Furthermore, the functions  $\Phi_H$ ,  $\Psi_H$ ,  $\Phi_L$ , and  $\Psi_L$  can be evaluated through fixing  $E$  and  $R$ , and changing  $\sigma_{yH}$ ,  $\sigma_{yL}$ ,  $n$ ,  $K$ ,  $E_i$ , and  $h_m$ . Table I lists the values or ranges for these parameters used in numerical calculations. Figures 1(a) and 1(b) show the finite element mesh used in this analysis. It consists of 6500 four-node axisymmetric elements. According to sensitivity evaluation, the mesh can adequately meet the requirement for simulating the behavior of a semi-infinite solid indented by a spherical indenter. Figures 2(a) and 2(b) and 3(a) and 3(b) show the functional relations of  $\Phi_H$ ,  $\Psi_H$ ,  $\Phi_L$ , and  $\Psi_L$ , respectively, with the condition of  $E_i/E = 373.3/70$  and  $h_m/R = 5/100$ .

Considering the Young's modulus  $E$  of tested material can be determined directly from the unloading curve of indentation tests,<sup>2</sup> in this research  $E$  as well as  $E_i$ ,  $R$ , and  $h_m$  are taken as known quantities. As the first approximation to true yield strength and hardening behavior, stress  $\sigma_{yH}$  and hardening exponent  $n$  or stress  $\sigma_{yL}$  and hardening modulus  $K$  can be determined from the combination of functions (8) and (9) or (10) and (11), provided that quantities  $P_m$  and  $X$  corresponding to an indentation depth  $h_m$  have been obtained from an indentation test. It is obvious that for the same indented material,  $P_m$  and  $X$  depend on  $h_m$ , so  $\sigma_{yH}$ ,  $n$ ,  $\sigma_{yL}$ , and  $K$  also depend on  $h_m$ . Here, three indentation depths are selected. They are  $h_m = 0.01R$ ,  $0.025R$ , and  $0.05R$ , and represented by symbol  $h_m^{(i)}$  ( $i = 1, 2$ , and  $3$ ). Correspondingly, the fitting load and exponent are represented by  $P_m^{(i)}$  and  $X^{(i)}$  ( $i = 1, 2$ , and  $3$ ), and the first approximate yield stresses

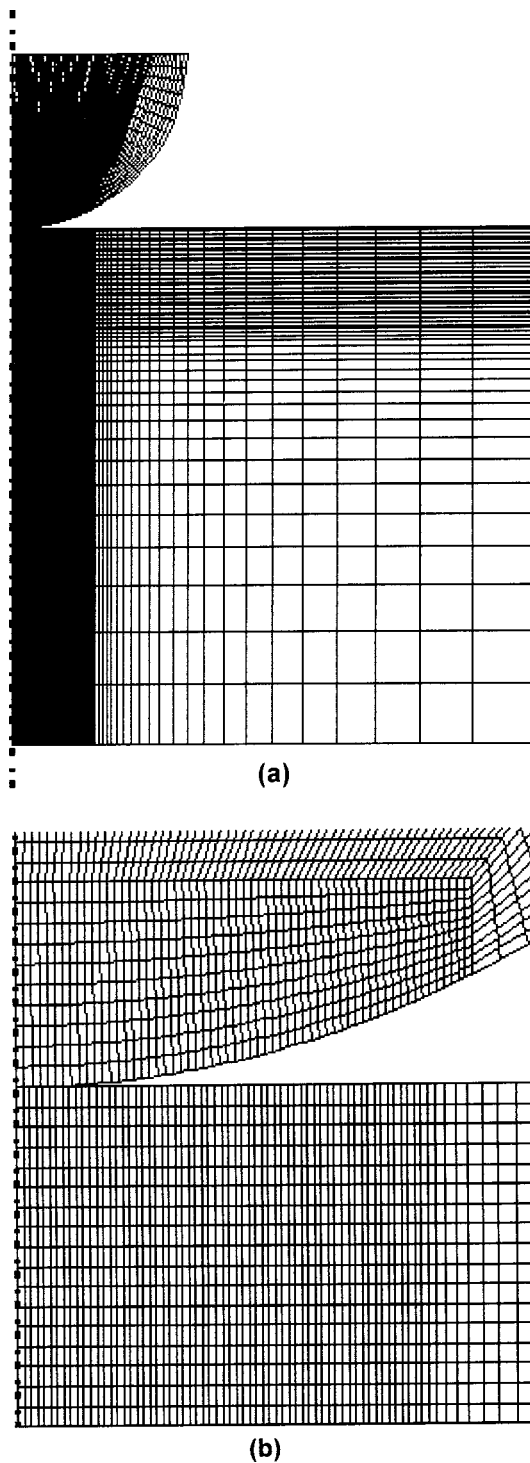


FIG. 1. (a) Overall finite element mesh; (b) detailed finite element mesh near the contact zone.

and hardening parameters are represented by  $\sigma_{yH}^{(i)}$ ,  $n^{(i)}$ ,  $\sigma_{yL}^{(i)}$ , and  $K^{(i)}$  ( $i = 1, 2, \text{ and } 3$ ). These data will be used to achieve the final and better estimation on the yield strength and hardening behavior.

### III. METHODOLOGY OF DETERMINING YIELD STRENGTH AND HARDENING BEHAVIOR

In order to make the proposed method applicable to wide material hardening behaviors, we consider the two typical

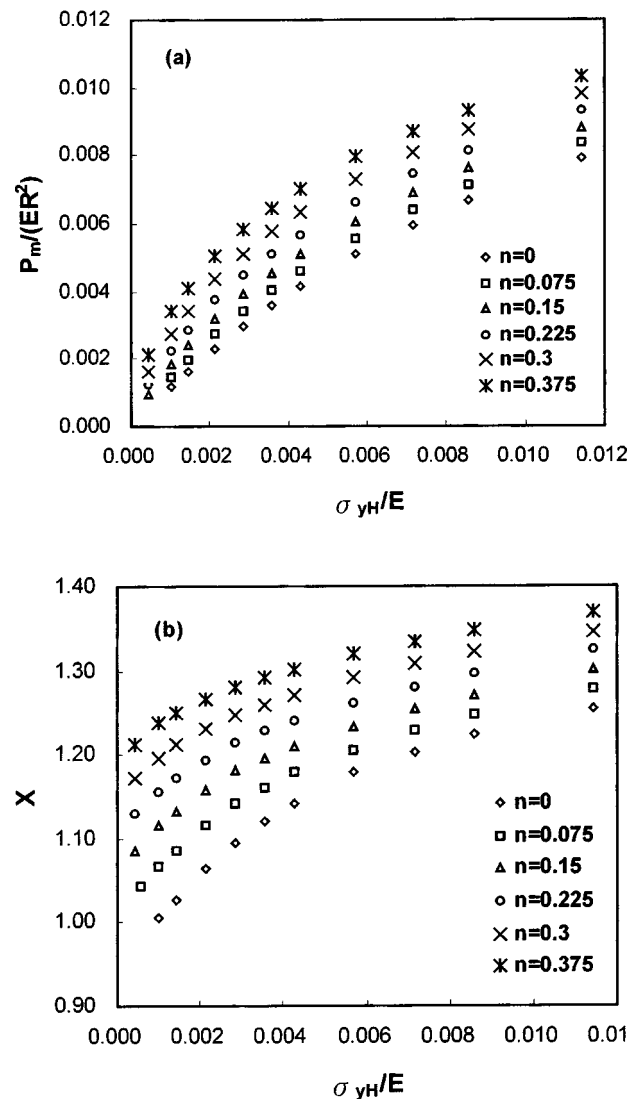


FIG. 2. (a)  $\sigma_{yH}/E$  and  $n$  dependence of  $P_m/(ER^2)$ , at  $E_i/E = 373.3/70$  and  $h_m/R = 5/100$ ; (b)  $\sigma_{yH}/E$  and  $n$  dependence of  $X$ , at  $E_i/E = 373.3/70$  and  $h_m/R = 5/100$ .

situations, i.e., the Hollomon's power law hardening and linear hardening mentioned in Sec. II. First, if the true hardening behavior of tested material obeys the former, the parameters  $\sigma_{yH}^{(i)}$  and  $n^{(i)}$  ( $i = 1, 2, \text{ and } 3$ ) determined from experimental data  $P_m^{(i)}$  and  $X^{(i)}$  ( $i = 1, 2, \text{ and } 3$ ) for three different depths  $h_m^{(i)}$  ( $i = 1, 2, \text{ and } 3$ ) should be the same, while the parameters  $\sigma_{yL}^{(i)}$  and  $K^{(i)}$  ( $i = 1, 2, \text{ and } 3$ ) determined from the same experiment should be different. The reason can be explained on the basis of the following fact. For the same tested material, the maximum equivalent plastic strain induced in the material depends on the maximum indentation depth, and the deeper the indentation depth, the larger the maximum equivalent plastic strain. In other words, the effective strain range in the stress-strain relation that influences the indentation response is different for different indentation depth. Therefore, in order to make linear hardening behavior equivalent to Hollomon's power law one [that is, the same values of  $P_m^{(i)}$  and  $X^{(i)}$  ( $i = 1, 2, \text{ and } 3$ ) can be obtained on the basis of the two different hardening behaviors] for different effective strain range, the parameters  $\sigma_{yL}^{(i)}$  and

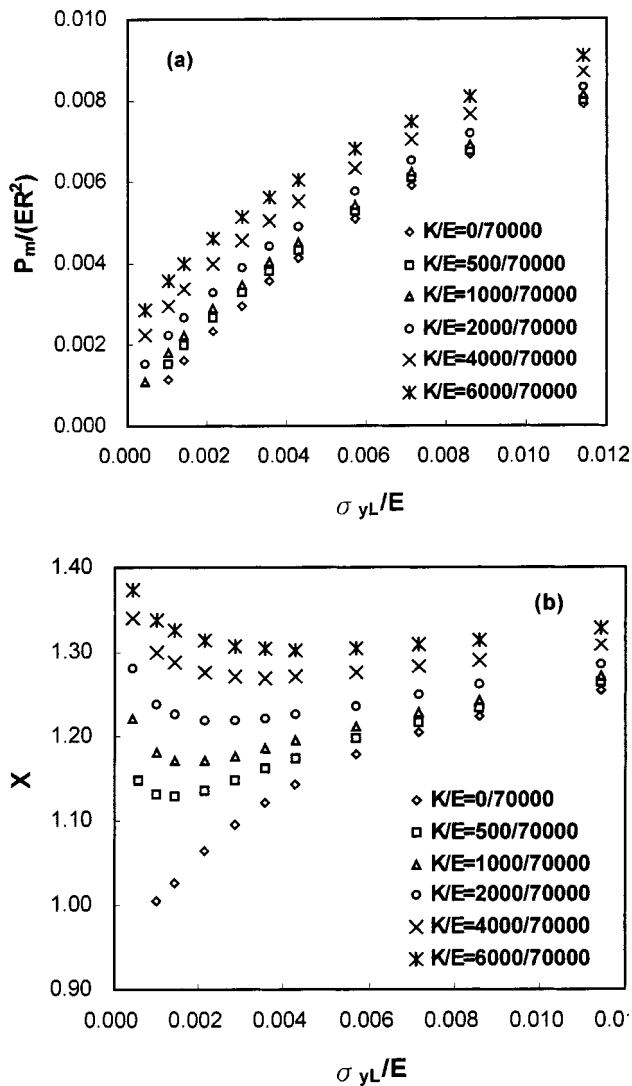


FIG. 3. (a)  $\sigma_{yL}/E$  and  $K/E$  dependence of  $P_m/(ER^2)$ , at  $E_i/E = 373.3/70$  and  $h_m/R = 5/100$ ; (b)  $\sigma_{yL}/E$  and  $K/E$  dependence of  $X$ , at  $E_i/E = 373.3/70$  and  $h_m/R = 5/100$ .

$K^{(i)}$  ( $i = 1, 2, \text{ and } 3$ ) need to take different values. The stress-strain relations for both elastic Hollomon's power law hardening with the same parameters  $\sigma_{yH}^{(i)}$  and  $n^{(i)}$  ( $i = 1, 2, \text{ and } 3$ ) and elastic-linear hardening with different parameters  $\sigma_{yL}$  and  $K^{(i)}$  ( $i = 1, 2, \text{ and } 3$ ) are illustrated in Fig. 4(a), where the intersecting points between the linear hardening lines  $L^{(i)}$  ( $i = 1, 2, \text{ and } 3$ ) and Hollomon's power law hardening curves  $H^{(i)}$  ( $i = 1, 2, \text{ and } 3$ ) determined at same indentation depth are defined as the characteristic points, which are represented by  $C_{ij}$ . Here, the first index  $i = 1, 2, \text{ and } 3$  corresponds to the three indentation depths  $h_m^{(i)}$ , and the second index  $j = 1 \text{ and } 2$  indicates the two intersecting points corresponding to the same maximum indentation depth. If the following power law function

$$\sigma = \alpha(\varepsilon + \varepsilon_0)^\beta \tag{12}$$

with three parameters  $\alpha$ ,  $\varepsilon_0$ , and  $\beta$ , i.e., Swift's power law hardening function is used to regress these six characteristic points  $C_{ij}$  ( $i = 1, 2, \text{ and } 3; j = 1 \text{ and } 2$ ), the finally determined hardening curve should approach the true one, i.e.,

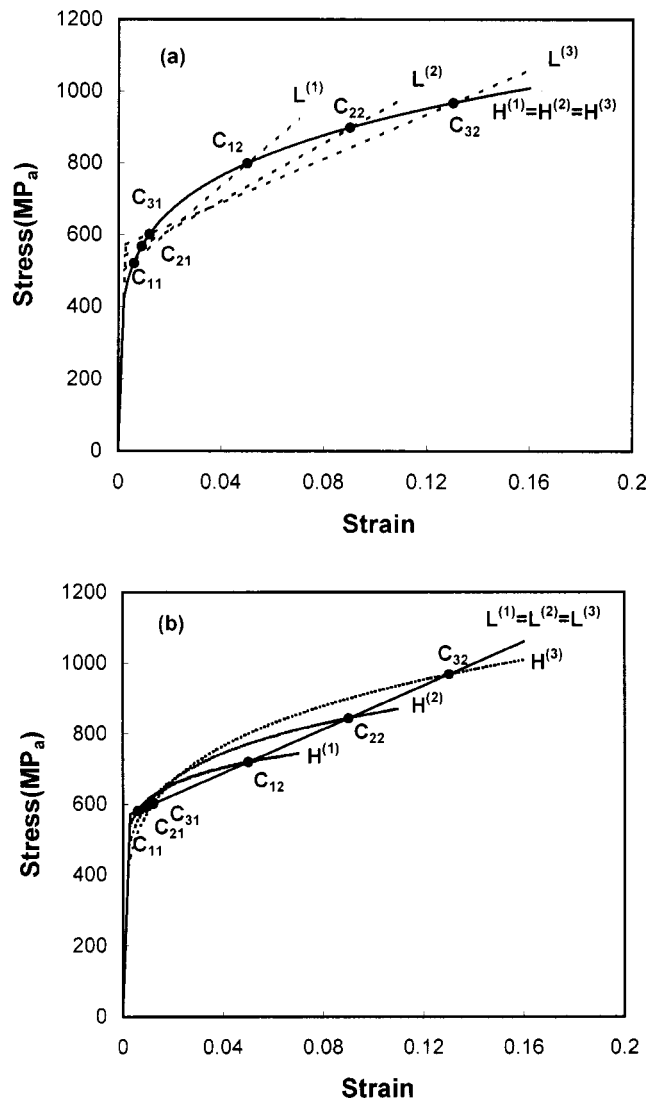


FIG. 4. (a) Generation of characteristic points by assuming a material to have pure elastic-Hollomon's power law hardening behavior; (b) generation of characteristic points by assuming a material to have pure elastic-linear hardening behavior.

Hollomon's power law. In fact, all of the six points  $C_{ij}$  ( $i = 1, 2, \text{ and } 3; j = 1 \text{ and } 2$ ) lie on the same Hollomon's power law hardening curve. Additionally, the yield strength determined by the combination of Eq. (12) and equation  $\sigma = E\varepsilon$  should approach the true one. Therefore, the characteristic points combined with equation  $\sigma = E\varepsilon$  and regression analysis using Swift's power law hardening function (12) can be applied to obtain the true yield strength and hardening behavior of Hollomon's hardening material.

Second, if the tested material obeys the linear hardening behavior, the parameters  $\sigma_{yL}^{(i)}$  and  $K^{(i)}$  ( $i = 1, 2, \text{ and } 3$ ) determined from experimental data  $P_m^{(i)}$  and  $X^{(i)}$  ( $i = 1, 2, \text{ and } 3$ ) for three different depths  $h_m^{(i)}$  ( $i = 1, 2, \text{ and } 3$ ) should be the same, while the parameters  $\sigma_{yH}^{(i)}$  and  $n^{(i)}$  ( $i = 1, 2, \text{ and } 3$ ) determined from the same experiment should be different, and the reason is similar to that explained for the first situation. Figure 4(b) shows the related stress-strain relations and the characteristic points  $C_{ij}$  ( $i = 1, 2, \text{ and } 3; j = 1 \text{ and } 2$ ) determined by the definition. Because these characteristic points

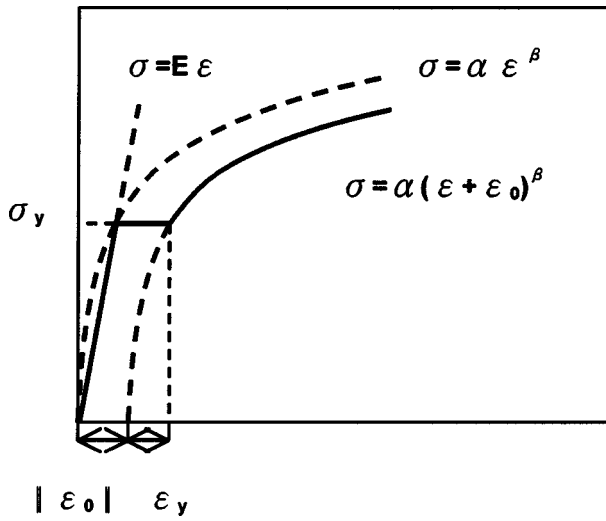


FIG. 5. Determination of stress-strain curve for the cases where  $\epsilon_0 < 0$ , corresponding to materials having an initial yield plateau.

lie on the same one linear hardening line, the true yield strength and hardening behavior can be obtained by applying the strategy used in the analysis for first situation. As a consequence, both Hollomon's power law hardening behavior and linear hardening behavior are identified by the same strategy. Therefore, to determine the yield strength and hardening behavior of wide materials with unknown hardening mode, it is natural to take the strategy as a general methodology, which consists of the following steps:

- (1) Selecting three indentation depths  $h_m^{(i)}$  ( $i = 1, 2, \text{ and } 3$ ) to make the ratios  $h_m^{(i)}/R$  ( $i = 1, 2, \text{ and } 3$ ) of 0.01, 0.025, 0.05, respectively.
- (2) Determining the values of  $P_m^{(i)}$  and  $X^{(i)}$  ( $i = 1, 2, \text{ and } 3$ ) by applying expression (3) to fit indentation loading curve of spherical indentation test with three indentation depths  $h_m^{(i)}$  ( $i = 1, 2, \text{ and } 3$ ).
- (3) Determining the first approximate yield stress  $\sigma_{yH}^{(i)}$  and hardening exponent  $n^{(i)}$  ( $i = 1, 2, \text{ and } 3$ ) by combining functions (8) and (9) based on the elastic-Hollomon's power law hardening behavior, as well as the first approximate yield stress  $\sigma_{yL}^{(i)}$  and hardening modulus  $K^{(i)}$  ( $i = 1, 2, \text{ and } 3$ ) by combining functions (10) and (11) based on the elastic-linear hardening behavior.
- (4) Calculating the coordinates of characteristic points  $C_{ij}$  ( $i = 1, 2, \text{ and } 3; j = 1 \text{ and } 2$ ) according to the definition of characteristic points and the parameters  $\sigma_{yH}^{(i)}$ ,  $n^{(i)}$ ,  $\sigma_{yL}^{(i)}$ , and  $K^{(i)}$  ( $i = 1, 2, \text{ and } 3$ ).

(5) Evaluating the parameters  $\alpha$ ,  $\beta$ , and  $\epsilon_0$  by regression analysis to the characteristic points  $C_{ij}$  ( $i = 1, 2, \text{ and } 3; j = 1 \text{ and } 2$ ) with the function (12).

(6) Determining the final estimate of the yield strength  $\sigma_y$  and hardening behavior according to two cases:

Case 1: If  $\epsilon_0 \geq 0$ ,  $\sigma_y$  is determined by combining the Eq. (12) and equation  $\sigma = E\epsilon$ , and the hardening behavior is expressed by:  $\sigma = \alpha(\epsilon + \epsilon_0)^\beta$ , for  $\epsilon \geq \epsilon_y = \sigma_y/E$ .

Case 2: If  $\epsilon_0 < 0$ , as shown in Fig. 5,  $\sigma_y$  is assigned to be the ordinate of the intersecting point between the curve  $\sigma = \alpha\epsilon^\beta$  and  $\sigma = E\epsilon$ . The stress strain relation is divided into three regions: (i)  $\sigma = E\epsilon$ , for  $\epsilon < \epsilon_y$ ; (ii)  $\sigma = \sigma_y$ ,

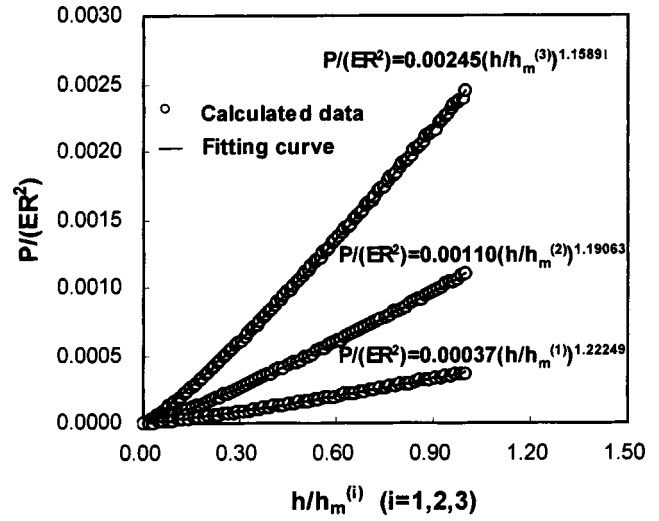


FIG. 6. Indentation loading curves of material S45C (Ref. 14) in dimensionless scales.

for  $\epsilon_y \leq \epsilon \leq \epsilon_y + \|\epsilon_0\|$ ; and (iii)  $\sigma = \alpha(\epsilon + \epsilon_0)^\beta$ , for  $\epsilon > \epsilon_y + \|\epsilon_0\|$ . Functions of this type are applicable to the materials with initial yield plateau.

#### IV. NUMERICAL VERIFICATION OF THE METHODOLOGY

Three groups of materials with known uniaxial stress-strain relations are selected to examine the proposed method. They are near linear hardening materials, near Hollomon's power law hardening materials, and the materials with initial yield plateau. If the Young's modulus and Poisson's ratio of all these materials take the same values of  $E = 210$  GPa and  $\nu = 0.3$ , respectively, and those of the spherical indenter take the values of  $E_i = 1120$  GPa and  $\nu_i = 0.2$ , respectively, the indentation loading curves for all of these materials can be obtained from finite element simulations. One of them is shown in Fig. 6, where both the calculated and fitting curves corresponding to three maximum indentation depths are depicted in dimensionless scales. Applying the methodology described in Sec. III, the yield strengths and hardening behaviors of all examined materials can be determined. The results together with the actual stress-strain relations and those evaluated under the condition of  $h_m/R = h_m^{(1)}/R = 0.01$  by the reported method,<sup>10</sup> which has the material behavior assumption of Hollomon's power law hardening, are all shown in Figs. 7(a)–7(f). In addition, the relative errors of the yield strengths determined by the two methods are given in Table II, in which  $\sigma_{yT}$  stands for the actual yield strength,  $\sigma_{yP}$  the estimated one by the present method, and  $\sigma_{yH}^{(i)}$  ( $i = 1, 2, \text{ and } 3$ ) the estimated ones by the reported method under the condition of different maximum indentation depths  $h_m^{(i)}/R = 0.01, 0.025, \text{ and } 0.05$  for  $i = 1, 2, \text{ and } 3$ . From the figures and table, it is evident that the proposed method can give good estimates of the yield strengths and hardening behaviors of a broad variety of materials, covering those with linear and Hollomon's power law hardening behaviors. Moreover, although some errors are observed when applying the method to the materials which exhibits an initial yield

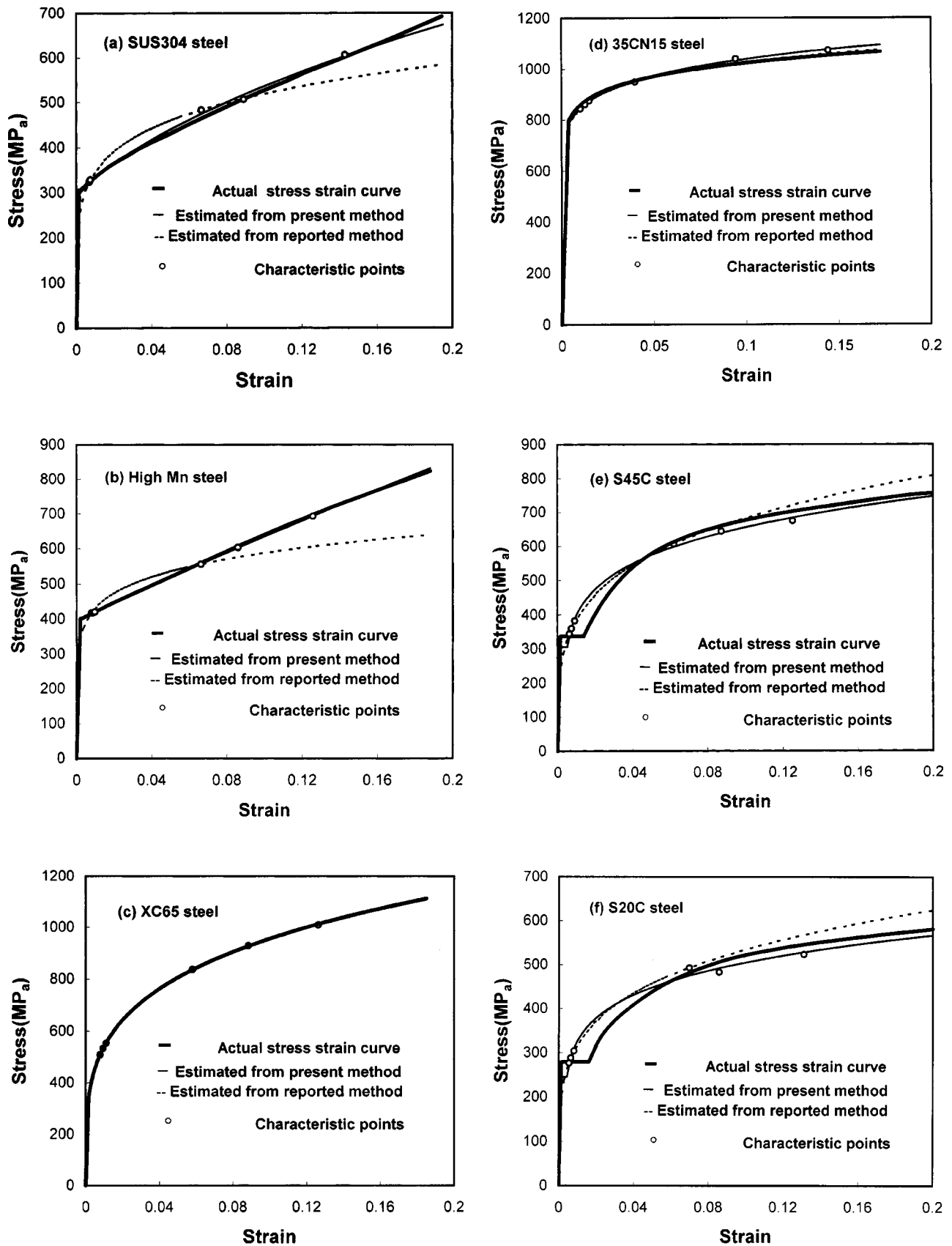


FIG. 7. (a) Estimated and actual stress-strain curves of SUS304 stainless steel (Ref. 15) with near linear-hardening behavior; (b) estimated and actual stress-strain curves of high Mn steel (Ref. 16) with near linear-hardening behavior; (c) estimated and actual stress-strain curves of XC65 steel (Ref. 10) with near Hollomon's power law hardening behavior; (d) estimated and actual stress-strain curves of 35CN15 steel (Ref. 10) with near Hollomon's power law hardening behavior; (e) estimated and actual stress-strain curves of S45C steel (Ref. 14) with initial yield plateau; (f) estimated and actual stress-strain curves of S20C steel (Ref. 17) with initial yield plateau.

TABLE II. Relative errors of yield strengths estimated by the present method and the reported method (unit of stress: MPa)

Materials	$\sigma_{yT}$	$\sigma_{yP}$	$\sigma_{yH}^{(1)}$	$\sigma_{yH}^{(2)}$	$\sigma_{yH}^{(3)}$	$(\sigma_{yT} - \sigma_{yP})/\sigma_{yP}$	$(\sigma_{yT} - \sigma_{yH}^{(1)})/\sigma_{yH}^{(1)}$	$(\sigma_{yT} - \sigma_{yH}^{(2)})/\sigma_{yH}^{(2)}$	$(\sigma_{yT} - \sigma_{yH}^{(3)})/\sigma_{yH}^{(3)}$
SUS304	301	307	236	236	218	-2%	28%	28%	38%
Mn steel	400	403	338	319	288	-1%	18%	25%	39%
XC65	345	358	349	347	347	-4%	-1%	-1%	-1%
35CN15	790	786	775	765	772	1%	2%	3%	2%
S45C	337	305	222	230	244	10%	52%	47%	38%
S20C	279	245	184	198	201	14%	52%	41%	39%

plateau, the deviations are reasonably small and acceptable from the engineering point of view. On the contrary, the abovementioned previously reported method is effective only for the near Hollomon's power law hardening materials. Considerably great errors could appear if it is applied to estimate the yield strengths for the materials not obeying ideal Hollomon's power law hardening behavior. Actually, considering the material hardening behavior assumptions underlying the methods, the results are not unexpected.

## V. CONCLUSIONS

A method for estimating yield strength and hardening behavior of metallic material from spherical indentation has been presented. The method is based on the conception of characteristic points proposed in this article. There are two crucial parts included in the procedure to fulfill the method. The first one is to determine the characteristic points corresponding to different maximum indentation depths. This can be achieved by determining the first approximate yield strengths and hardening behaviors from the spherical indentation loading curve of tested material and the numerical relationships established to relate separate material hardening properties and indentation responses by means of dimensional and finite element analysis. The second one is to carry out the regression analysis to the characteristic points using Swift's power law function with three parameters. As a remarkable advantage, the utilization of the characteristic points makes the proposed method applicable to wide variety of materials exhibiting separate hardening behaviors. This has been demonstrated by the examination to three groups of materials with near linear hardening behavior, near Hollomon's power law hardening behavior, and initial yield plateau.

According to the finite element analysis of spherical indentation performed by Mesarovic and Fleck,<sup>9</sup> the friction between the indenter and the indented material has a negligible effect on the load-displacement relationship for a shallow indentation of  $h_m/R \leq 0.05$ . Therefore, the validity of the present method would not be affected by the level of interfacial friction.

## ACKNOWLEDGMENTS

This work was supported by the Center for Smart Materials of the Hong Kong Polytechnic University (Code: 1.A.310) and a Hong Kong ITF Fund (Code: K.11.2A.ZP07).

- <sup>1</sup>J. B. Pethica, R. Hutchings, and W. C. Oliver, *Philos. Mag. A* **48**, 593 (1983).
- <sup>2</sup>W. C. Oliver and G. M. Pharr, *J. Mater. Res.* **7**, 1564 (1992).
- <sup>3</sup>J. Gubicza, A. Juhasz, and J. Lendvai, *J. Mater. Res.* **11**, 2964 (1996).
- <sup>4</sup>J. S. Field and M. V. Swain, *J. Mater. Res.* **10**, 101 (1995).
- <sup>5</sup>Y.-M. Chen, A. W. Ruff, and J. W. Dally, *J. Mater. Res.* **9**, 1314 (1994).
- <sup>6</sup>F. M. Haggag, *ASTM STP* **1204**, 27 (1993).
- <sup>7</sup>J. Alcalá, A. E. Giannakopoulos, and S. Suresh, *J. Mater. Res.* **13**, 1390 (1998).
- <sup>8</sup>Y.-T. Cheng and C.-M. Cheng, *J. Mater. Res.* **14**, 3493 (1999).
- <sup>9</sup>S. Dj. Mesarovic and N. A. Fleck, *Proc. R. Soc. London* **455**, 2707 (1999).
- <sup>10</sup>A. Nayebe, R. E. Abdi, O. Bartier, and G. Mauvoisin, *Mech. Mater.* **34**, 243 (2002).
- <sup>11</sup>M. Beghini, L. Bertini, and V. Fontanari, *Int. J. Comp. Appl. Tech.* **15**, 168 (2002).
- <sup>12</sup>S. Kucharski and Z. Mroz, *Mater. Sci. Eng.* **318**, 65 (2001).
- <sup>13</sup>ABAQUS, Version 6.2, Hibbit, Karlsson, & Sorensen, Inc. (Pawtucket, RI 02860).
- <sup>14</sup>Y. Murakami and K. Matsuda, *ASME J. Appl. Mech.* **61**, 822 (1994).
- <sup>15</sup>Y. Tomita and Y. Shibutani, *Int. J. Plasma* **16**, 769 (2000).
- <sup>16</sup>M. Huang, *The Mechanical Properties of Metals* (Xi'an Jiaotong University Press, Xi'an, 1986) (in Chinese).
- <sup>17</sup>Y. Murakami and L. P. Yuan, *J. T. Eva.* **20**, 15(1992).